Effects of Flexibility in the Bearing Assemblies of Dual-Spin Spacecraft

M. P. SCHER*
TRW Systems Group, Redondo Beach, Calif.

The recent performance of a dual-spin spacecraft suggests that bearing assembly flexibility may affect the stability of desired attitude motions. The present analysis confirms this possibility for certain dual-spin spacecraft whose bearing assemblies dissipate energy during lateral bending. Energy sink techniques are used to derive an approximate time constant for the growth or decay of coning of the spacecraft's symmetry axis; and the accuracy of this expression is assessed by means of computer simulations. It is also seen that the time constant can be bounded, even without complete knowledge of the dissipation mechanism, and a useful design guideline is thus obtained. Examination of the sign of the time constant provides a criterion that facilitates stability analyses of spacecraft with dissipators on either the rotor or platform; charts of stability regions are presented.

I. Introduction

Dual-Spin Spacecraft

IN recent years, several investigators have studied the stability of attitude motions of dual-spin spacecraft. These spacecraft are comprised of two sections that rotate relative to one another about an axis fixed with respect to both. Typically, one section, called the rotor, is symmetric about this axis and rotates rapidly relative to the second section, or platform, whose angular velocity in inertial space is much smaller in magnitude. The sections are separated by a bearing assembly consisting of an axle, bearings, and a motor. Such spacecraft are well-suited to certain missions because the rotor can provide spin-stabilization to maintain the common axis in a fixed orientation in inertial space, while the motor torque cancels the frictional torques between the sections, thereby keeping the platform de-spun, i.e., at rest as regards rotational motion.

The aforementioned stability analyses[1–5] have established that it is indeed possible to design a dual-spin spacecraft whose common axis will maintain a fixed orientation in inertial space. However, this will only occur when certain relationships, involving the inertia properties, spin rates, and flexible members of the rotor and platform are maintained. In particular, it has been shown that the platform and the common axis can remain rotationally at rest, even when the centroidal moment of inertia of the entire spacecraft about a line normal to the common axis exceeds the spacecraft's moment of inertia about that axis, provided that the rate of energy dissipation on the platform exceeds that on the rotor by a sufficient amount. This conclusion was announced by Iorillo,[1] and was later enlarged upon by Likins,[2] for the case where dissipation occurs on both sections of the spacecraft. These investigations relied heavily on admittedly informal energy sink arguments, but a more rigorous Floquet analysis, leading to essentially the same conclusion for a specific system, was presented by Mingori.[3] In addition, the conclusion has been supported by numerous other rigorous analyses in which only one of the sections was regarded as nonrgid,[2–4] and by numerical integrations of exact dynamical equations for the motion of spacecraft with dissipators on both sections.[5]

Presented as Paper 70-1043 at the AAS/AIAA Astrodynamics Conference, Santa Barbara, Calif., August 19–21, 1970; submitted September 18, 1970; revision received January 15, 1971.

* Member of Technical Staff, Applied Mechanics Laboratory. Member AIAA.

Practical Considerations

The importance of this conclusion regarding the stability of dual-spin spacecraft whose common axes are principal axes of minimum inertia is three-fold. First, it is clear that dual-spin spacecraft are not subject to the widely accepted doctrine which states that, in the presence of energy dissipation, a single-body spacecraft may only spin in a stable fashion about its centroidal principal axis of maximum inertia. Second, it permits dual-spin spacecraft to be rod-shaped, rather than disk-shaped, thereby effectively utilizing the available space on present launch vehicles. Third, criteria for stability in terms of energy dissipation rates prove extremely useful in the actual spacecraft design process. Analysts can estimate the rates at which energy is dissipated by various phenomena such as fuel slosh and structural damping. Those dissipative phenomena found to be most significant can later be incorporated into computer simulations that deal rigorously with the dynamical interactions of the various parts of the spacecraft. Moreover, when it is found that additional energy dissipation would be desirable, the engineer may design a passive wobble damper to meet dissipation requirements without having to cope with the complete nonlinear equations for the spacecraft's attitude motion.

Surprisingly, the first dual-spin spacecraft to which this conclusion was applied exhibited occasional periods of insta-

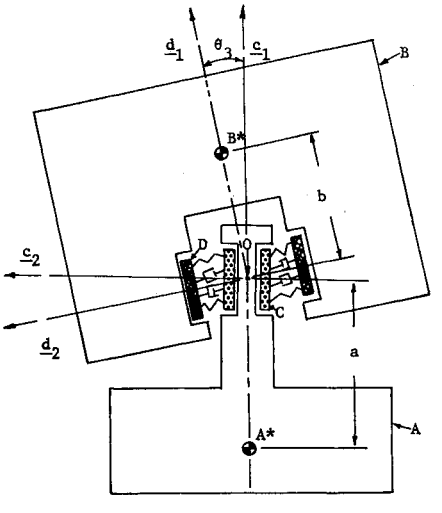

Fig. 1 Symmetric dual-spin spacecraft with flexible bushing.

bility during which the rotor's symmetry axis was observed to be coning about an inertially fixed line with a small cone angle. Subsequent investigations, conducted to explain this instability, have identified nonrigidity in the bearing assembly as a probable cause.[6] Flexibility in lateral bending apparently permitted energy to be dissipated through viscous flow of lubricant between a bearing race and axle. This eventuality was not adequately assessed prior to launch. A complete hypothesis as to why coning was limited to a small angle hinges on nonlinearities in the bearing assembly and on interactions with the active control system, and is beyond the scope of the present paper. However, the incident does point out the need for analytical methods with which to predict the effects of bearing assembly flexibility on spacecraft attitude motion and to provide design criteria for future bearing assemblies. The present paper attempts to treat both of these problems.

II. Results

Model

Analysis of the effects of bearing assembly flexibility is hampered by two major obstacles. First, it is not clear what phenomena should be analyzed. Bearing assemblies are intricate devices exhibiting nonlinearities in their moment-deflection characteristics and having complex patterns of lubricant flow among the bearings and races. Moreover, there are significant variations among the assembly designs used on different spacecraft, so an accurate model of a specific bearing assembly is of limited applicability. The second obstacle is that the aforementioned stability analyses treat only simplified spacecraft having ideal bearings. Consequently, it is not clear whether energy dissipation in the bearings should be attributed to the rotor or to the platform or, perhaps, apportioned in some manner between the two sections.

The present paper circumvents the first obstacle by considering the simplest relevant model of a compliant bearing assembly, i.e., by assuming 1) that the bending occurs at only one point and 2) that the restoring and damping forces in the assembly are proportional to the deflection and rate of deflection, respectively. The question of apportioning energy is avoided by modeling a system in which the dissipating mechanism is tied to neither the rotor nor the platform. This is accomplished by considering a symmetric spacecraft whose rotor and platform are separated by a massless, viscoelastic bushing which rotates at constant rates relative to both sections. The system is shown in Fig. 1 in which A and B are axisymmetric rigid bodies representing the platform and rotor and having mass centers A^* and B^*, respectively. The bushing is comprised of two symmetric massless annuli C and D, connected by idealized springs and dashpots that resist bending of D relative to C about any line passing through 0 and normal to the symmetry axes of C and D. Axial rotation of D relative to C is prohibited.

Typically, it might be desired that the system remain unflexed and that the symmetry axis remain fixed in space while A spins at a rate s (in inertial space) about this axis and while B spins relative to A about the axis with a rate Ω. (One may let A be de-spun by setting $s = 0$.) C and D, as a unit, may also be allowed to rotate relative to A about the symmetry axis with a rate $r\Omega$. Thus, if $r = 0$, C and D are fixed relative to A; and if $r = 1$, they are fixed in B. Values of r between zero and one are meaningful as long as a bushing is being considered; e.g., it might be assumed that the bushing rotates relative to A with a rate $\frac{1}{2}\ \Omega$. However, the principal role of the parameter r is to serve as an apportioning factor. By performing laboratory tests of actual bearing assemblies, it may be possible to empirically determine an appropriate value of r for a physical system that bears little resemblance to the bushing presently being analyzed.

Now, if the spacecraft's symmetry axis is coning about an inertially fixed line (parallel to the spacecraft's angular momentum vector), the bushing must transmit torques applied by B to A. These torques cause bending, which, in turn, leads to viscous dissipation in the bushing. In the sequel, the spacecraft will be termed stable if the analysis indicates that the coning and, hence, the bending diminish. On the other hand, instability is manifested by increased bending and coning.

Time Constant

The rate at which the cone angle increases or decays can be most easily characterized by a time constant T, a positive value of T being defined as the time required for the cone angle to decrease by a factor of $1/e$. An estimate of this time constant has been derived by employing energy sink techniques which, as indicated previously, sacrifice a certain amount of rigor, but in turn provide a convenient closed-form expression for T. A review of this derivation, and of the underlying assumptions, follows shortly, but for now it suffices to indicate that the techniques involve 1) obtaining an analytical description of the motion which the spacecraft undergoes while coning, 2) recognizing that the bushing is excited by this motion in a periodic fashion, 3) computing the energy dissipated per excitation cycle, and 4) relating energy changes to attitude changes. The outcome of this procedure can be presented in terms of the following parameters characterizing the system: I = moment of inertia of the entire system about the symmetry axis (when unflexed); J = moment of inertia of the entire system about any line through the system mass center and normal to the symmetry axis (when unflexed); B_1 = moment of inertia of B about its symmetry axis; B_2 = moment of inertia of B about a line normal to its symmetry axis and passing through B^*; m_A = mass of A; m_B = mass of B; a = distance from A^* to 0; b = distance from B^* to 0; k = spring constant for lateral bending about 0; c = damping coefficient for lateral bending about 0; s = nominal spin rate of A in inertial space; Ω = nominal spin rate of B relative to A; and r = ratio of spin rate of C in A to nominal spin rate of B in A.

If one defines

$$M = m_A m_B/(m_A + m_B) \tag{1}$$

$$\alpha = I/J \qquad \rho = s/\Omega \tag{2a}$$

$$\beta_1 = B_1/J \qquad \beta_2 = [B_2 + Mb(a + b)]/J \tag{2b}$$

$$\eta = c/J\Omega \qquad \Lambda = \rho(\alpha\beta_2 - \beta_1) + \beta_1(\beta_2 - 1) \tag{2c}$$

$$\sigma = k/J\Omega^2 \tag{3}$$

and

$$\lambda = \rho(\alpha - 1) + \beta_1 - r \tag{4}$$

then T may be estimated as

$$T = [(\sigma^2 + \lambda^2\eta^2)/\Lambda^2\eta(\alpha\rho + \beta_1)\lambda]/\Omega \tag{5}$$

All the terms of importance in the model appear in this expression for T; e.g., the spring and damping coefficients enter via σ and η. Note that the magnitude of the time constant can always be made infinitely large by the choice of an infinite spring stiffness. (Of course, actual spacecraft have other sources of dissipation whose time constant contributions become dominant when the bearings become sufficiently stiff.) The rate of rotation of the bushing enters Eq. (5) via λ, which plays an important role in the analysis, $\lambda\Omega$ being the frequency with which the bushing is excited. In fact α, β_1, ρ, and r may be chosen such that λ vanishes, in which case the bushing is not flexed in an oscillatory fashion and T becomes infinite.

The accuracy of this time constant expression has been assessed by comparing values predicted by Eq. (5) with those

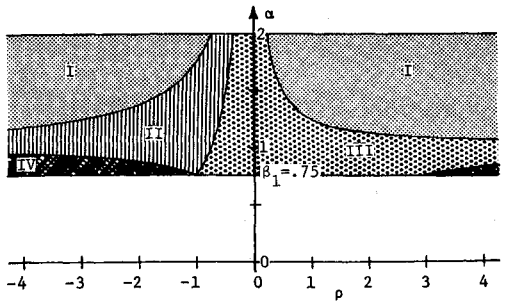

Fig. 2 Stability chart when $\beta_1 = 0.75$.

obtained by numerical (computer) integration of a complete set of equations of motion for the spacecraft. These equations were linearized in the angles that describe the bending, but not in the angular rates. The bushing was always taken to be fixed relative to the platform ($r = 0$). Values of time constants were extracted from the numerical time histories of the platform's inertial angular velocity components by measuring the time required for the magnitude of the transverse rates to diminish by 37%. In Table 1, such comparisons are presented for three dual-spin spacecraft configurations. The first two configurations represent spacecraft with large rotors and small de-spun platforms, the first having $\beta_1 > 1$ and the second with $\beta_1 < 1$. [The significance of β_1 will soon be made apparent; e.g., see Eq. (7).] The third spacecraft has a slowly spinning platform and a small disk-shaped rotor.

For each spacecraft, and for various values of σ and η, the ratio T/T^* is presented where T is the value of the time constant as given by Eq. (5) and T^* is the value obtained from the numerical integration. In addition, Table 1 presents the ratio P/P^* where P, the analytically predicted period of a cycle of bending, is defined as $2\pi/\lambda\Omega$, and P^* is the oscillation period determined numerically. (All values of η were chosen to be optimal, i.e., to minimize $|T|$, except those indicated by the footnote.) It can be seen that the analytical predictions usually improve with increasing spring and damping coefficients. Note also that, in most cases, Eq. (5) underestimates the value of T. When σ is small, differences between P and P^* become large. This indicates that the excitation frequency seen by the bushing differs from that assumed in the derivation of Eq. (5); thus, accurate estimates of T cannot be expected when the bushing is highly flexible.

Table 1 Comparison of analytical predictions and numerical integrations

σ	η	T/T^*	P/P^*
Spacecraft properties: $\alpha = 0.9$ $\beta_1 = 0.8$ $\beta_2 = 0.6$ $\rho = 0$ $r = 0$			
0.3	0.375	0.78	0.83
3.0	3.75	0.99	0.98
30.0	37.5	0.96	0.99
3.0	1.0[a]	0.93	0.97
3.0	10.0[a]	1.00	0.99
Spacecraft properties: $\alpha = 1.2$ $\beta_1 = 1.1$ $\beta_2 = 0.8$ $\rho = 0$ $r = 0$			
0.15	0.136	1.06	0.71
1.5	1.36	1.06	0.98
15.0	13.6	0.98	0.99
Spacecraft properties: $\alpha = 1.5$ $\beta_1 = 0.2$ $\beta_2 = 0.1$ $\rho = 0.1$ $r = 0$			
0.45	0.3[a]	0.65	0.91
0.45	1.8	0.85	0.94
1.5	6.0	0.95	1.00

[a] Nonoptimal η for a given σ.

Stability

In using Eq. (5), it is convenient to choose $\Omega > 0$. Then stability is indicated if

$$(\alpha\rho + \beta_1)\lambda > 0 \tag{6}$$

a criterion which depends only on the inertia properties I, J, B_1 and on the spin rates s, Ω, $r\Omega$, of the platform, rotor, and bushing. The term stability is meant to imply only that $T > 0$. This loose treatment of stability is necessary in lieu of a rigorous stability analysis of the system's nonlinear dynamical equations which are by-passed in the present approach. Nevertheless, when r equals zero or one, Eq. (6) does agree with stability criteria developed by more rigorous methods.[3,4]

For a spacecraft having its platform de-spun, $s = \rho = 0$, and Eq. (6) may be replaced by

$$\beta_1 - r > 0 \tag{7}$$

Note that if the dissipator is fixed relative to the platform ($r = 0$), then stability is always assured, whereas, if the dissipator is fixed to the rotor ($r = 1$), then β_1 must exceed unity to insure stability.

Equation (6) may also be used to shed some light on the general questions of stability of dual-spin spacecraft. By examining the (α,β_1,ρ) parameter space for the cases where $r = 0$ and $r = 1$, one can develop charts of stability domains.[3] These charts indicate whether platform-mounted and rotor-mounted dissipators contribute to stability or instability. Three such charts are presented in Figs. 2–4 for the cases where $\beta_1 = 0.75$, 1.0, and 1.25, respectively. In each case, for a given β_1, the values of α and ρ are bounded by the inequalities $-\infty < \rho < \infty$ and $\beta_1 < \alpha < 2$; and the (α,ρ) parameter space is divided into regions which may be of four types as follows: type I—those regions in which stability is expected both when $r = 0$ and when $r = 1$; type II—those regions in which stability is expected when $r = 1$, but not when $r = 0$; type III—those regions in which stability is expected when $r = 0$, but not when $r = 1$; and type IV—those regions in which instability is expected both when $r = 0$ and when $r = 1$.

Notice that only when $\beta_1 < 1$ (i.e., in Fig. 2) does a type IV region appear; however, when the platform is de-spun ($\rho =$

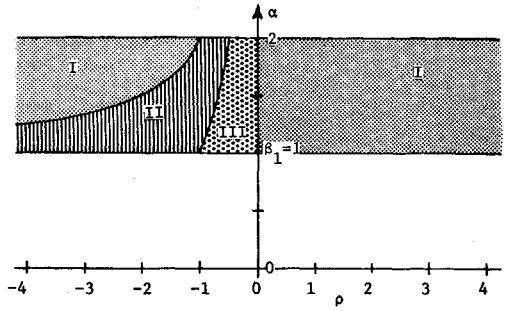

Fig. 3 Stability chart when $\beta_1 = 1.0$.

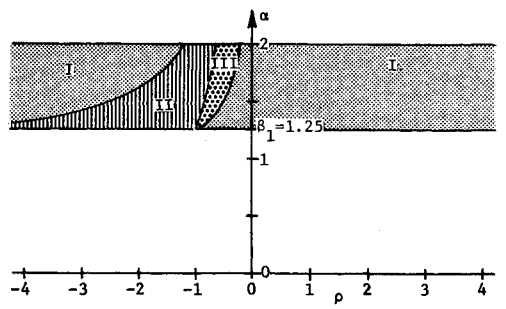

Fig. 4 Stability chart when $\beta_1 = 1.25$.

0), this region can be avoided. Figure 3 is perhaps only of academic interest since it is impossible to build a spacecraft with an inertia ratio β_1 of exactly 1.0. This case is unique in that a boundary between two regions occurs when $\rho = 0$. Thus, if dissipation on the rotor is dominant, stability can be obtained when the platform rotates slowly in the same direction as the rotor, but not if it is slowly counter-rotating. Finally, when $\beta_1 > 1$, as in Fig. 4, a spacecraft with a de-spun platform is stable regardless of dissipator location; however, instabilities do arise when the platform is counter-rotating at appropriate rates, both when a dissipator is fixed to the rotor and when one is fixed to the platform.

Bounding Analyses

The principal motivation for resorting to energy sink techniques is to obtain results that are of use in the design process. Unfortunately, exploitation of Eq. (5) presupposes knowledge of k, c, and r. Routinely, k is determined from static deflection tests of actual bearing assemblies; however, only more complicated experiments can furnish suitable values of c and r. In lieu of these values, one can, by differentiation of Eq. (5), determine that value of η which minimizes $|T|$; subsequent substitution into Eq. (5) produces

$$|T|_{\min} = 2\sigma/[\Lambda^2|\Omega(\alpha\rho + \beta_1)|] \tag{8}$$

Furthermore, from inspection of Eq. (5) it is evident that the maximum possible value of $|T|$ is infinite, i.e., when $\eta = 0$ or ∞. Thus $|T|$ can be bounded with respect to η without any knowledge of c and, moreover, these bounds are independent of r.

In the design process, one usually possesses an estimate of a stabilizing time constant provided by a wobble damper or active control system. It might then be asked how stiff need the bearing assembly be in order that, in no case, can there exist a destablizing time constant whose magnitude is less than T_0. If Eq. (6) is not satisfied for all values of r between 0 and 1, then a destabilizing time constant may occur. The minimum nondimensional stiffness that assures $|T| \geq |T_0|$ may be extracted from Eq. (8), after replacing $|T|_{\min}$ by T_0, i.e.,

$$\sigma_{\min} = \tfrac{1}{2}\Lambda^2|\Omega T_0(\alpha\rho + \beta_1)|$$

and the minimum stiffness k follows from Eq. (3).

It is expected that stiffnesses that are predicted in this manner may be overly conservative, perhaps by one or more orders of magnitude, depending on the actual values of c and r that are bypassed in this bounding analysis. If weight limitations prohibit such conservative stiffnesses, a more flexible bearing assembly can be designed and subjected to laboratory tests to determine the values of c and r.

III. Derivation

Quasi-Rigid Body Motion

A derivation of Eq. (5) is now presented based on the assumption that the attitude motion of the spacecraft is not greatly affected during one cycle of bending in the bushing; but over longer times, the cumulative effect of bushing flexibility on attitude motion must be considered. The analysis proceeds in four steps, the first being the determination of the translational and rotational motions which body A undergoes assuming that 1) there is no flexibility in the bushing, 2) no external forces act on the spacecraft, and 3) the symmetry axis of the spacecraft is coning about the spacecraft's inertially fixed angular momentum vector. Consideration of the rotational motion of A is then most easily accomplished by invoking the dynamic equation

$$\dot{\mathbf{H}} = 0 \tag{9}$$

in which the dot denotes time differentiation in an inertial reference frame and $\mathbf{H}$, the angular momentum of the spacecraft about its mass center S^*, can be expressed as

$$\mathbf{H} = (I\omega_1 + B_1\Omega)\mathbf{c}_1 + J\omega_2\mathbf{c}_2 + J\omega_3\mathbf{c}_3 \tag{10}$$

where $\mathbf{c}_1,\mathbf{c}_2,\mathbf{c}_3$ are unit vectors fixed in C with $\mathbf{c}_1$ parallel to the symmetry axis of A (see Fig. 1), and where $\omega_1,\omega_2,\omega_3$ are measure numbers of $\boldsymbol{\omega}^A$, the inertial angular velocity of A, referred to $\mathbf{c}_1,\mathbf{c}_2,\mathbf{c}_3$, i.e.,

$$\boldsymbol{\omega}^A = \omega_1\mathbf{c}_1 + \omega_2\mathbf{c}_2 + \omega_3\mathbf{c}_3 \tag{11}$$

The differentiation indicated in Eq. (9) can be expanded as

$$\dot{\mathbf{H}} = \mathbf{H}' + \boldsymbol{\omega}^C \times \mathbf{H} \tag{12}$$

where the prime denotes vector differentiation with respect to time in reference frame C, and $\boldsymbol{\omega}^C$, the inertial angular velocity of C, is given by

$$\boldsymbol{\omega}^C = \boldsymbol{\omega}^A + r\Omega\mathbf{c}_1 \tag{13}$$

Execution of the operations in Eq. (12), taking $\mathbf{H}$ from Eq. (10) and regarding Ω as constant and $\omega_1,\omega_2,\omega_3$ as time dependent, leads to three scalar differential equations which, for appropriate initial conditions, have the solutions

$$\omega_1 = s \qquad \omega_2 = \omega_t \cos\lambda\Omega t \qquad \omega_3 = \omega_t \sin\lambda\Omega t \tag{14}$$

where s and ω_t are constants referred to as the spin rate and transverse rate of A, respectively, and λ is given by Eq. (4). Next, by employing the definition of mass center, the inertial acceleration $\mathbf{a}_A$ of A^* relative to S^*, can be expressed in terms of $\mathbf{r}$, the position vector of B^* relative to A^*, as $\mathbf{a}_A = -\ddot{\mathbf{r}}m_B/(m_A + m_B)$ or, after noting from Fig. 1 that $\mathbf{r} = (a + b)\mathbf{c}_1$ when the spacecraft is unflexed, as

$$\mathbf{a}_A = \frac{m_B}{m_A + m_B}(a + b)\{[\omega_2^2 + \omega_3^2]\mathbf{c}_1 - [\dot{\omega}_3 + (\omega_1 + \Omega r)\omega_2]\mathbf{c}_2 + [\dot{\omega}_2 - (\omega_1 + \Omega r)\omega_3]\mathbf{c}_3\} \tag{15}$$

Bending of the Bushing

The second step in the procedure is to determine the bending motion of the bushing, i.e., the motion of D relative to C, assuming 1) that flexing of the bushing has a negligible effect on the motion of A [i.e., that $\boldsymbol{\omega}^A$ and $\mathbf{a}_A$ are given by Eqs. (14) and (15)], 2) that bending of the bushing occurs only at point O, and 3) that the bending is small. Equations that govern the bending can most easily be developed by applying the vectorial form of Euler's equations for the rotational motion of a single rigid body to platform A, namely

$$\mathbf{M}^A = \mathbf{I}^A\cdot\dot{\boldsymbol{\omega}}^A + \boldsymbol{\omega}^A \times \mathbf{I}^A\cdot\boldsymbol{\omega}^A \tag{16}$$

where $\mathbf{M}^A$ is the moment about A^* of the forces applied to A and $\mathbf{I}^A$, the inertia dyadic of A for A^*, may be expressed as

$$\mathbf{I}^A = A_1\mathbf{c}_1\mathbf{c}_1 + A_2\mathbf{c}_2\mathbf{c}_2 + A_2\mathbf{c}_3\mathbf{c}_3 \tag{17}$$

A_1 and A_2 being the centroidal longitudinal and transverse principal moments of inertia of A. Now, $\mathbf{M}^A$ is dependent, in part, on the bending of D relative to C. If three mutually perpendicular unit vectors, $\mathbf{d}_1$, $\mathbf{d}_2$, $\mathbf{d}_3$, are fixed in D so that they are aligned with $\mathbf{c}_1$, $\mathbf{c}_2$, $\mathbf{c}_3$ when the bushing is unflexed, then the orientation of D relative to C during bending can be described by successive rotations of amounts θ_2 and θ_3 about $\mathbf{c}_2$ and $\mathbf{d}_3$; and, assuming bending is small so that $\cos\theta_i \simeq 1$, $\sin\theta_i \simeq \theta_i$ then these unit vectors are related as follows:

$$\mathbf{d}_1 = \mathbf{c}_1 + \theta_3\mathbf{c}_2 - \theta_2\mathbf{c}_3,\ \mathbf{d}_2 = -\theta_3\mathbf{c}_1 + \mathbf{c}_2,\ \mathbf{d}_3 = \theta_2\mathbf{c}_1 + \mathbf{c}_3 \tag{18}$$

When bending occurs,

$$\mathbf{M}^A = -(k\theta_2 + c\dot{\theta}_2)\mathbf{c}_2 - (k\theta_3 + c\dot{\theta}_3)\mathbf{d}_3 + T_1{}^A\mathbf{c}_1 + ac_1 \times \mathbf{F}^A \tag{19}$$

where T_1^A is the sum of the motor and frictional torques applied to A and where $\mathbf{F}^A$, the force exerted by C on A (and assumed to pass through O), may be expressed using Newton's law as

$$\mathbf{F}^A = m_A \mathbf{a}_A \tag{20}$$

Next, dot multiplication of Eq. (16) by $\mathbf{c}_2$ and by $\mathbf{c}_3$ and substitution from Eqs. (1, 11, 13, 15, 17–20) leads to two scalar equation of motion

$$(\dot{\omega}_2 - r\Omega\omega_3)[A_2 + Ma(a+b)] + \omega_1\omega_3[A_1 - A_2 - Ma(a+b)] = k\theta_2 + c\dot{\theta}_2$$
$$(\dot{\omega}_3 + r\Omega\omega_2)[A_2 + Ma(a+b)] - \omega_1\omega_2[A_1 - A_2 - Ma(a+b)] = k\theta_3 + c\dot{\theta}_3 \tag{21}$$

Now, letting the bending of the bushing produce no effect on the angular motion of A, Eqs. (14) may be substituted into Eq. (21) and, after recognizing that

$$I = A_1 + B_1 \qquad J = A_2 + B_2 + M(a+b)^2 \tag{22}$$

defining

$$\tau = \Omega t \qquad \xi = \omega_t/\Omega \tag{23}$$

designating scalar differentiation with respect to τ by a prime, and recalling the definitions in Eqs. (2–4), Eqs. (21) can be reduced to the system

$$\eta\theta_2' + \sigma\theta_2 = \xi\Lambda \sin\lambda\tau, \quad \eta\theta_3' + \sigma\theta_3 = -\xi\Lambda\cos\lambda\tau \tag{24}$$

which has a steady-state solution for the bending angles θ_2 and θ_3, given by

$$\theta_2 = u\sin\lambda\tau - v\cos\lambda\tau, \quad \theta_3 = v\sin\lambda\tau - u\cos\lambda\tau \tag{25}$$

where

$$u = \xi\Lambda\sigma/(\sigma^2 + \eta^2\lambda^2) \qquad v = \xi\Lambda\eta\lambda/(\sigma^2 + \eta^2\lambda^2) \tag{26}$$

It can be seen from Eqs. (24) that the forcing functions for the bending angles have frequencies of $\lambda\Omega$ and, hence, are dependent on r. Use of the steady-state solution given by Eq. (25) is based on the implicit assumption that the transient solutions to Eq. (24) are unimportant. This can be expected when the natural frequency of the bushing in lateral bending is far removed from this forcing frequency and when sufficient damping is present.

Energy Dissipation Rate

The third step in the procedure is to compute the rate at which energy is dissipated in the bushing, assuming that the bending of D relative to C is described by θ_2 and θ_3 of Eqs. (25). Examination of Eqs. (25) and (23) reveals that the bending angles oscillate with a period P given by

$$P = 2\pi/\lambda\Omega \tag{27}$$

The energy E dissipated per cycle is given by

$$E = \int_0^P c(\dot{\theta}_2^2 + \dot{\theta}_3^2)dt \tag{28}$$

and $\dot{K}_b^*$, the average rate of energy dissipation, is defined as $\dot{K}_b^* = -E/P$ or, after substitution from Eqs. (23–28) and (2), by

$$\dot{K}_b^* = J\Omega^3\eta\lambda^2\Lambda^2\xi^2/(\sigma^2 + \eta^2\lambda^2) \tag{29}$$

This expression can be used in its present form to calculate the rage of energy dissipation in the bushing when comparison with the dissipation rates of other phenomena is desired; alternately, it can be used to determine T of Eq. (5) as will next be seen. In any event, note that $\dot{K}_b^*$ is proportional to the square of ω_t; when there is no coning motion, ω_t and $\dot{K}_b^*$ both vanish.

Changes in Attitude Motion

The fourth and final step is to relate energy dissipation rates to changes in attitude motion. The primary assumptions involved are that 1) bending is small; 2) in the spirit of variation of parameters, ω_1 and ω_t are allowed to vary slowly; and 3) that the coning angle of the symmetry axis of A is small or, equivalently, that ω_t is small. Because it has been assumed that C and D rotate at constant rates relative to A and B, respectively, one must hypothesize the existence of two power sources (e.g., motors), which maintain these constant rates, adding or removing mechanical energy as necessary. Thus, $\dot{K}$, the rate of change of kinetic energy of the entire spacecraft, is comprised of three parts, i.e.,

$$\dot{K} = \dot{K}_b + \dot{K}_A + \dot{K}_B \tag{30}$$

where $\dot{K}_b$ is the instantaneous rate of energy dissipation in the bushing and $\dot{K}_A$ and $\dot{K}_B$ are rates at which energy is added to the system by the motors attached to A and B, respectively. Now, the total system energy can be related to the attitude motion as follow: first, the bushing is treated as rigid, in which case the spacecraft's kinetic energy is given by

$$K = \tfrac{1}{2}(I\omega_1^2 + 2B_1\omega_1\Omega + B_1\Omega^2 + J\omega_t^2) \tag{31}$$

and the square of the angular momentum is obtained from Eq. (10) as

$$\mathbf{H}^2 = I^2\omega_1^2 + 2IB_1\omega_1\Omega + B_1^2\Omega^2 + J^2\omega_t^2 \tag{32}$$

Elimination of ω_1 between Eqs. (31) and (32), followed by time differentiation in which $\mathbf{H}^2$ and Ω are regarded as constants, leads to

$$\dot{K} = (J/I)(I - J)\omega_t\dot{\omega}_t \tag{33}$$

Thus, the rate of change of system kinetic energy is related to the transverse rate. Next, the rates at which energy is provided by the motors can be identified as

$$\dot{K}_A = \mathbf{M}^A \cdot {}^C\boldsymbol{\omega}^A \qquad \dot{K}_B = \mathbf{M}^B \cdot {}^D\boldsymbol{\omega}^B \tag{34}$$

where $\mathbf{M}^A$ and $\mathbf{M}^B$ are the moments of the forces applied by C and D to A and B about A^* and B^*, respectively; and ${}^C\boldsymbol{\omega}^A$ and ${}^D\boldsymbol{\omega}^B$ are the respective angular velocities of A and B relative to C and D, i.e.,

$${}^C\boldsymbol{\omega}^A = -r\Omega\mathbf{c}_1 \qquad {}^D\boldsymbol{\omega}^B = (1 - r)\Omega\mathbf{d}_1 \tag{35}$$

Now, Euler's equations, applied successively to A and to B, together with small coning and bending assumptions that permit the dropping of terms quadratic in ω_2, ω_3, θ_2, and θ_3, provide that

$$\mathbf{M}^A \cdot \mathbf{c}_1 = A_1\dot{\omega}_1 \qquad \mathbf{M}^B \cdot \mathbf{d}_1 = B_1\dot{\omega}_1 \tag{36}$$

and $\dot{\omega}_1$ and $\dot{\omega}_t$ may be related by differentiating Eq. (32) as

$$\dot{\omega}_1 = -J^2\omega_t\dot{\omega}_t/[I(I\omega_1 + \Omega B_1)] \tag{37}$$

Rearrangement of Eq. (30), followed by substitution from Eqs. (33–37, 2, 4, and 22–23) and replacement of ω_1 by s, leads to

$$\dot{K}_b = J\Omega^3[\lambda/(\alpha\rho + \beta_1)]\xi\xi'$$

an expression which relates the rate of energy dissipation in the bushing to the rate of change of the (nondimensional) transverse rate. The crux of the energy sink approach involves equating $\dot{K}_b$ to $\dot{K}_b^*$ of Eq. (29), thus leading to a differential equation for ξ, i.e.,

$$\xi' + [\eta\Lambda^2(\alpha\rho + \beta_1)\lambda/(\sigma^2 + \lambda^2\eta^2)]\xi = 0$$

having the solution

$$\xi = \xi_0 e^{-\tau/\Omega T} \tag{38}$$

where ξ_0 is a constant that depends on initial conditions, and T is the time constant presented in Eq. (5). Recalling the

definitions of ξ and τ from Eq. (23), Eq. (38) indicates that ω_t, and hence the coning angle, grows or decays depending on the sign of T.

References

[1] Iorillo, A. J., "Nutation Damping Dynamics of Axisymmetric Rotor Stabilized Satellites," ASME Winter Meeting, Chicago, Ill., Nov. 1959.

[2] Likins, P. W., "Attitude Stability Criteria for Dual Spin Spacecraft," *Journal of Spacecraft and Rockets*, Vol. 4, No. 12, Dec. 1967, pp. 1638–1643.

[3] Mingori, D. L., "Effects of Energy Dissipation on the Attitude Stability of Dual-Spin Satellites," *AIAA Journal*, Vol. 7, No. 1, Jan. 1969, pp. 20–27.

[4] Pringle, R., Jr., "Stability of the Force-Free Motions of a Dual-Spin Spacecraft," *AIAA Journal*, Vol. 7, No. 6, June 1969, pp. 1054–1063.

[5] Velman, J. R., "Simulation Results for a Dual-Spin Spacecraft," *Proceedings of the Symposium on Attitude Stabilization and Control of Dual-Spin Spacecraft, Aug. 1–2, 1967*, Rept. SAMSO-TR-68-191, Nov. 1967, U. S. Air Force.

[6] Johnson, C. R., "Tacasat I Nutation Dynamics," to be published in *AIAA Progress in Astronautics and Aeronautics: Communications Satellite Technology for the 70's*, Vol. 25, edited by N. E. Feldman and C. M. Kelly, MIT Press, Cambridge, 1971.

MAY 1971 AIAA JOURNAL VOL. 9, NO. 5

Large Deformation, Deep Penetration Theory for a Compressible Strain-Hardening Target Material

SATHYA HANAGUD*
Georgia Institute of Technology, Atlanta, Ga.

AND

BERNARD ROSS†
Failure Analysis Associates, Stanford, Calif.

Hypervelocity impact of a rigid spherical projectile with a compressible target material is investigated. Analytic solutions obtained for this problem are based on dynamic cavity expansion and Goodier deep penetration theories and are not restricted, as in previous work, to an incompressible medium. Target compressibility is introduced through a locking approximation for real material behavior under hydrostatic stress. In particular, values of locking density are obtained from Hugoniot curves characterizing homogeneous, isotropic material behavior at different impact velocities. Results of the theory indicate that terminal penetration depth is a function of projectile diameter and mass, and initial density, locking density, yield stress, and strain-hardening modulus of the target material. Using results of the theory, curves are plotted to show the comparison between compressible and incompressible penetration theory for the hypervelocity impact of steel projectiles on an aluminum target.

Nomenclature

A,D,M = cross section area, diameter, and mass of projectile, respectively
a = radius of spherical cavity
B_1,B_2 = constants related to dynamic pressure, see Eq. (71)
b = radius of locked-elastic, locked-plastic spherical shock front
C_1 = constant of integration
E,G = modulus of elasticity and shear modulus, respectively
E_t = tangent modulus for linear strain-hardening
e = bulk strain
$\bar{f}$ = limit of integration
f,g = functions of integration
k = radius of stress-free, locked-elastic spherical shock front
n = summation exponent
p_s = static pressure term given by Eq. (71)
$p(t)$ = dynamic pressure applied to spherical cavity surface as a function of time
$q,\dot{q},\ddot{q}$ = depth, velocity, and acceleration, respectively, of projectile in target material
q_0,v_0 = penetration depth and velocity of projectile after completion of shallow penetration phase
q_t = final penetration depth of projectile
r = Eulerian radial coordinate
t = time
v = outward particle velocity in radial direction
Y = yield stress
α = material constant given by Eqs. (16), (24)
β = material constant given by Eq. (40)
δ = material constant given by Eq. (66)
ϵ_1,ϵ_2 = small quantities in the mathematical sense
$\bar{\epsilon}_l$ = locking strain, $\bar{\epsilon}_l = -\epsilon_l$
$\epsilon_r,\epsilon_\theta$ = normal strains in radial and circumferential directions, respectively
η = series expression given by Eq. (54)
θ,φ = equatorial and meridional spherical coordinates, respectively
ρ,ρ_l = density and locking density of target material, respectively
σ_r,σ_θ = normal stresses inr adial and circumferential directions, respectively

Received January 26, 1970; revision received November 19, 1970. Work supported by the Naval Ordnance Laboratory, White Oak, Md. and the Office of Naval Research.

* Professor of Aerospace Engineering, (visiting), formerly Research Mathematician, Stanford Research Institute, Menlo Park, Calif., and at present a Senior Consultant to the Failure Analysis Associates.

† Engineer, Structural Mechanics, formerly Engineering Physicist, Stanford Research Institute, Menlo Park, Calif. Member AIAA.